Assessment of long-term deformation of a tunnel in soft rock by utilizing particle swarm optimized neural network

Kovačević, Meho Saša ; Bačić, Mario; Gavin, Kenneth; Stipanovič, Irina

DOI
10.1016/j.tust.2021.103838

Publication date
2021

Document Version
Final published version

Published in
Tunnelling and Underground Space Technology

Tunnelling and Underground Space Technology 110 (2021) 103838

Contents lists available at ScienceDirect

Tunnelling and Underground Space Technology incorporating Trenchless Technology Research

journal homepage: www.elsevier.com/locate/tust

Assessment of long-term deformation of a tunnel in soft rock by utilizing particle swarm optimized neural network

Meho Saša Kovačević [a], Mario Bačić [a,*], Kenneth Gavin [b], Irina Stipanović [c]

[a] University of Zagreb, Faculty of Civil Engineering, Department of Geotechnics, fra Andrije Kačića Miošića, 26 10 000 Zagreb, Croatia
[b] TU Delft, Faculty of Civil Engineering and Geosciences, Stevinweg 1/PO box 5048, 2628 CN Delft/2600 GA Delft, Netherlands
[c] University of Twente, Faculty of Engineering Technology, Drienerlolaan 5, 7522 NB Enschede, Netherlands

ARTICLE INFO

Keywords:
Soft rock tunneling
Long-term deformation
Rheological parameters
Neural network
Particle swarm optimization
Tunnel monitoring

ABSTRACT

The continuous monitoring of long-term performance of tunnels constructed in soft rock masses shows that the rock mass deformations continue after construction, albeit at a rate that reduces with time. This is in contrast with NATM postulates which assume deformation stabilizes shortly after tunnel construction. This paper proposes the prediction of long-term vertical settlement performance of a tunnel in soft rock mass, through the inclusion of a Burger's creep viscous-plastic constitutive law to model post-construction deformations. To overcome issues related to the complex characterization of this constitutive model, a neural network NetRHEO is developed and trained on a numerically obtained dataset. A particle swarm algorithm is then employed to estimate the most probable rheological parameter set, by utilizing the long-term in-situ monitoring data from several observation points on a real tunnel. The paper demonstrates the potential of the proposed methodology, using displacement measurements of two adjacent tunnels in karstic rock mass in Croatia. The complex interaction of a railway tunnel Brajdica and a road tunnel Pećine, conditioned by the character of the surrounding rock mass as well by the chronology of their construction, was evaluated to predict the future behavior of these tunnels.

1. Introduction

The establishment of a novel philosophy in tunnel construction, the New Austrian Tunneling Method (NATM), marked a turning point in the mindset of tunneling engineers (Carranza-Torres and Fairhurst, 1999; Oreste, 2003). The method relies on achieving optimum safety and economy in tunnel construction, by utilizing the natural phenomenon of activation of the rock mass load bearing function. One of the method's basic principles considers that a rock mass surrounding tunnel should be substantially stabilized by the primary support, leading to relatively small deformations after the tunnel construction. This is important having in mind that excessive ground movements may result in damage to adjacent buildings and utilities (Goh et al., 2016), or yielding due to excessive internal forces within the tunnel lining system (Zhang et al., 2020a). Though it is difficult in such a complex system to ensure that deformations are completed at the end of the tunnel excavation process, as redistribution of stresses occur around the completed tunnel, the assumption is that the resultant settlement are small and occur in a relatively short time period.

However, this assumption may not be true when tunneling in soft rock, such are soluble karstic rock masses. These exhibit strain softening behavior and time-dependent features, leading to creep settlement and induced squeezing. The term "squeezing" originates from the pioneering days of tunneling through the Alps, with the ISRM defining "squeezing of rock" as time dependent convergence or deformation that may terminate during construction or continue over a long period of time. Therefore, squeezing phenomena can lead to significant reduction of a cross section during construction, as reported by Barla et al. (2008) for the railway tunnel on Lyon-Torino line, see Fig. 1a, or it can occur long after the construction, as it was the case of a road tunnel in Japan where significant squeezing-induced uplift occurred 17 years after the end of construction (Okui et al., 2012), see Fig. 1b. Thus long-term squeezing can lead to long-term settlement problems and even delayed failure of structure, such as the case of the Laerdal tunnel in Norway, where failure of the shotcrete failure occurred nearly four years after its excavation (Grimstad, 2001).

The scientific community is well-aware of the long-term deformation phenomenon, and this research domain attracts continued attention

* Corresponding author.
E-mail addresses: msk@grad.hr (M.S. Kovačević), mbacic@grad.hr (M. Bačić), K.G.Gavin@tudelft.nl (K. Gavin), i.stipanovic@utwente.nl (I. Stipanović).

https://doi.org/10.1016/j.tust.2021.103838
Received 2 July 2020; Received in revised form 28 December 2020; Accepted 29 December 2020
Available online 22 January 2021

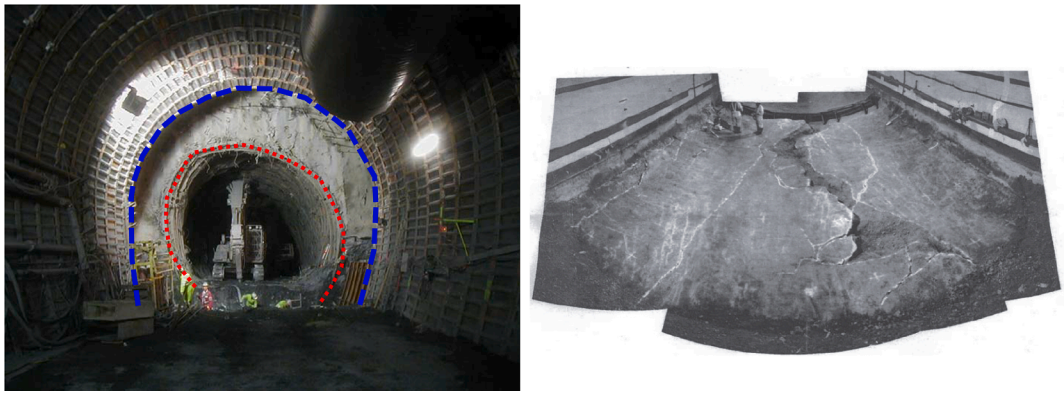

Fig. 1. Squeezing-induced reduction of a cross section during construction Lyon-Torino tunnel, from Barla et al. (2008) (a), and squeezing-induced uplift of tunnel's inverted arch long after the construction of tunnel in Japan from Okui et al. (2012) (b).

(Schubert et al., 2003; Barla et al., 2008; Guan et al., 2009; Xu et al. 2012). Arapov et al. (2009) and Kovačević et al. (2018) have conducted continuous long-term measurements of deformations of karstic rock mass surrounding the tunnels and have shown that there are significant differences between measured deformations and those anticipated in design. The measured deformations are significantly higher than those obtained through calculations, while the measured trends of deformations differ from those estimated. Therefore, it is evident that time-dependent features of soft rock behavior should be considered in tunnel design.

Despite the existing awareness of delayed deformations and their influence on tunnel construction and exploitation, prediction of long – term behavior is not a simple task due to very complex evaluation of time-dependent rheological parameters. This evaluation could be conducted through extensive laboratory tests as suggested by Aydan et al. (2014), including the specified creep, relaxation and quasi-static compression tests (Maranini and Brignoli 1999; Li and Xia, 2000; Fabre and Pellet, 2006). However, these tests are usually of high cost and long duration. Boidy et al. (2002) note that rock properties, determined from laboratory tests, cannot be directly used for prediction of tunnel behavior for appropriate numerical simulations and it is essential to compare simulation results with obtained measurements from monitoring the tunnels over a long period. While there is still much to learn in order to properly define parameters which would describe long-term creep behavior of a rock mass, in-situ long-term monitoring seems to have a vital role in this process. Eurocode 7 (CEN, 2004) recommends monitoring more than ten years after construction is complete, or throughout the life of the structure, where failure may result in abnormal risks to property and life. One of the very well documented examples is the tunnel Ureshino line I in Japan, where the long term monitoring results obtained during the tunnel exploitation were utilized for the development of advanced constitutive models describing the long term behavior of rock mass (Guan et al., 2008), as well as for developing a methodology of rheological parameter estimation (Guan et al., 2009).

This paper presents an approach to predict the long-term behavior of tunnels excavated in soft rocks. The estimation of rheological parameters for a modified Burgers constitutive model is conducted by using a neural network, as proposed by the Guan et al. (2009), while the selection of the most probable set of rheological parameters was done by the means of particle swarm algorithm, PSO. To increase the estimation precision, data from instrumentation that monitored the tunnel deformation at various depths below ground level and over a period of several years was utilized. The overall methodology is verified at a case study location in Croatia, where long–term monitoring data of a road tunnel Pećine was used to evaluate its complex interaction with an adjacent 100 year old railway tunnel Brajdica, that was recently reconstructed by widening its cross section.

2. A constitutive representation of time-dependent deformations

Several factors influence the long - term deformation of rock mass and these include the geological history, initial stress field, mineralogy, discontinuity orientation, construction technology and tunneling method, rate, support type, etc. The long-term deformation alone is the result of a series of complex processes such as creep of the intact rock, creep of material fill between discontinuities and delayed development of new cracks. After the development of instantaneous deformations due to the excavation of the tunnel opening, the rock mass reaches a state of primary creep, in which deformations occur with a rate that reduces in

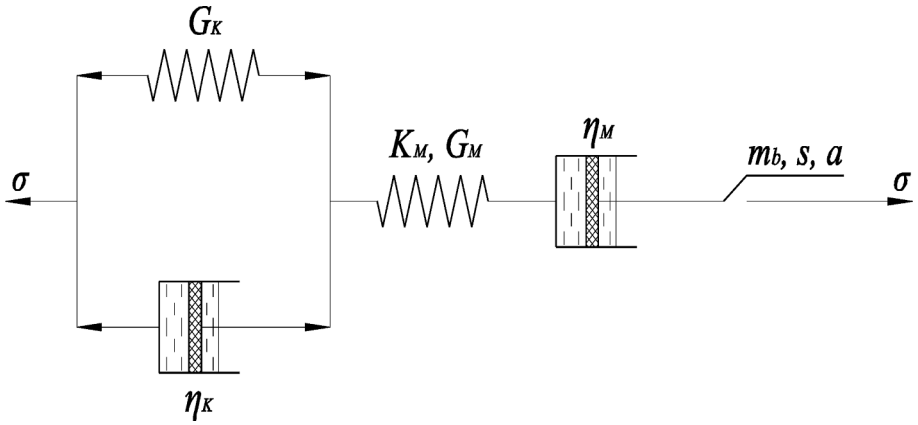

Fig. 2. A classic Burgers-creep visco-plastic model with implemented Hoek-Brown plastic law (modified from Itasca, 2019).

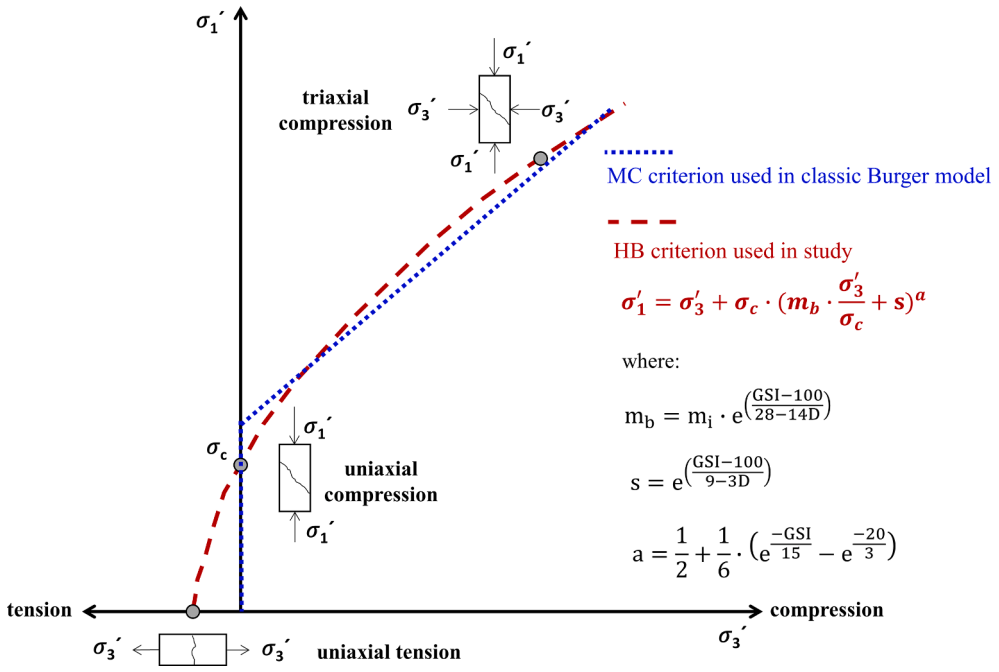

Fig. 3. Comparison of the MC and HB failure criteria.

time. This phase is followed by a secondary creep process, characterized by a constant deformation rate and by a tertiary creep characterized by an increase in rock mass deformation rates over time (Xue et al., 2014), eventually leading to the progressive damage and collapse of the rock mass.

A number of constitutive models have been proposed to account for the time-dependent features of rock masses (Jin and Cristescu, 1998; Pellet et al., 2005; Shao et al., 2006; Guan et al., 2008; Lv et al., 2019). One of the most common types are the visco-plastic models in which the constitutive laws form a relation between the current strain rate to the current stress and/or stress rate. These relationships can be schematically represented by a spring, dashpot and plastic slider that are connected in parallel and/or in series. One such constitutive model is the classic Burgers-creep visco-plastic model, characterized by a visco-elasto plastic deviatoric behavior and elasto-plastic volumetric behavior. The visco-elastic and plastic strain-rate components are assumed to act in series, see Fig. 2. A Kelvin unit is characterized by shear modulus G_K and viscosity η_K, while a Maxwell unit is characterized by elastic shear modulus G_M, Maxwell viscosity η_M and Maxwell bulk modulus K_M.

The plastic constitutive law of a classic Burger's model utilizes the Mohr-Coulomb failure criteria, represented by cohesion (c), friction angle (ϕ) and dilation (ψ), connected in series and subjected to a certain deviatoric loading jointly. However, the plastic element of a classic Burger's model was modified within this study to consider the non-linear nature of rock mass by implementation of Hoek-Brown (HB) strength criteria (Hoek and Torres, 2002). This criterion is described by the m_b, s and a empirical parameters and it offers advantages in the determination of the overall strength of in-situ rock masses, especially when it comes to soft rock masses.

Deviatoric strain rate partitioning can be formulated as:

$$\dot{e}_{ij} = \dot{e}_{ij}^{K} + \dot{e}_{ij}^{M} + \dot{e}_{ij}^{P} \tag{1}$$

The constitutive laws of the deviatoric behavior for three parts of Burger's model are:

$$s_{ij} = 2\eta^{K}\dot{e}_{ij}^{K} + 2G^{K}e_{ij}^{K} \tag{2}$$

$$\dot{e}_{ij}^{M} = \frac{\dot{s}_{ij}}{2G^{M}} + \frac{s_{ij}}{2\eta^{M}} \tag{3}$$

$$\dot{e}_{ij}^{P} = \lambda\frac{\partial g}{\partial\sigma_{ij}} - \frac{\dot{\varepsilon}_{kk}^{P}}{3}\delta_{ij} \text{ where } \dot{\varepsilon}_{kk}^{P} = \lambda\left(\frac{\partial g}{\partial\sigma_{11}} + \frac{\partial g}{\partial\sigma_{22}} + \frac{\partial g}{\partial\sigma_{33}}\right) \tag{4}$$

where e_{ij} are deviatoric components derived from strain tensor, s_{ij} are deviatoric components derived from stress tensor, ε_{kk} are volumetric components of strain tensor and σ_{kk} are volumetric components of stress tensor. The variables with dot mark refer to their first differential with respect to rheological time. The superscripts K, M and P denote the Kelvin, Maxwell, and HB plastic components of the corresponding variables. A λ is a multiplier that can be eliminated in the calculation afterwards.

The constitutive laws of volumetric behavior can be formulated as:

$$\dot{\sigma}_{kk} = 3K(\dot{\varepsilon}_{kk} - \dot{\varepsilon}_{kk}^{P}) \tag{5}$$

The envelope of the stress state is defined by the HB failure criterion, with the failure criterion f having the form:

$$f = \sigma'_1 - \sigma'_3 - \sigma_c\left(m_b\frac{\sigma'_1}{\sigma_c} + s\right)^a \tag{6}$$

where σ_1' is the maximum effective principal stress, σ_3' is the minimum effective principal stress. Determination of this criteria requires the knowledge of the uniaxial compression strength of the intact rock (*UCS*, sometimes referred to as σ_c); Geological Strength Index (*GSI*) representing the rock mass quality data which may be systematically collected and evaluated during site investigation, as well as during tunnel construction; factor D as the disturbance factor quantifying the disturbance effect over rock mass due to excavations; and the rock-type constant m_i, see Fig. 3.

To provide a relation between the components of strain rate at failure, a plastic potential g has similar form as the failure criterion:

$$g = \sigma'_1 - \sigma'_3 - \sigma_c\left(m_{dil}\frac{\sigma'_1}{\sigma_c} + s\right)^a \tag{7}$$

The plastic potential function based on dilation parameter m_{dil} rangers from 0 to m_b / 4 as suggested by Deb (2010), where m_{dil} being less than m_b makes the flow rule non-associated. If $m_{dil} = m_b$, the flow rule is associated, as it was applied in this study. The modified Bruger's constitutive model with HB plastic element, is implemented in

numerical analysis of this study by means of two-dimensional finite difference software FLAC (Itasca, 2019) and its programming language FISH.

3. Estimation of rheological parameters by using the particle swarm optimization algorithm

To numerically describe the different elements of the given constitutive model, their proper evaluation is of upmost importance. Some of the parameters, such as the Maxwell bulk modulus K_M and shear modulus G_M, density ρ and strength empirical m_b, s and a parameters can be determined through the standard laboratory and/or field investigation works.

When it comes to bulk modulus K_M, it can be determined through the well-known correlations with rock mass deformation Young modulus:

$$K_M = \frac{E_{rm}}{3 \times (1 - 2\nu)} \tag{8}$$

and same goes for Maxwell shear modulus G_M:

$$G_M = \frac{E_{rm}}{2 \times (1 + \nu)} \tag{9}$$

with E_{rm} being rock mass deformation modulus and ν as Poisson's coefficient. Kovačević et al. (2011) present intensive measurements from projects undertaken in karstic soft rock that show significantly higher measured rock mass deformations values than suggested by moduli correlated with rock mass classifications. Based on these observations, Jurić Kaćunić et al. (2011) developed a new approach for determination of the karst carbonate rock deformation modulus, given by Eq. (10):

$$E_{rm} = ID_m \times GSI^2 \times V_p{}^2 \tag{10}$$

where E_{rm} is in (GPa), geological strength index GSI is in (%) and the dispersion velocity of longitudinal waves V_p is in (km/s). The rock mass deformation index (ID_m) for carbonate rocks is equal to the rock mass quality index (IQ_s) determined by allocating rock mass into one of the proposed models and weathering zones, whereas the geological strength index (GSI) is adapted to the geological engineering properties of Croatian karst (Pollak, 2007). The strength parameters can be determined from UCS and GSI as shown in Fig. 3.

However, a challenge arises when trying to quantitatively estimate the time-dependent parameters G_K, η_K and η_M of modified Burger's model. As an alternative to high cost and the long duration rheological laboratory tests, this study offers a solution in form of utilization of neural network along with application of Particle Swarm Optimization (PSO) algorithm. For this purpose, the three unknowns are defined:

- ratio of Kelvin shear modulus and Maxwell bulk modulus: G_K/K_M
- Kelvin viscosity: η_K
- Maxwell viscosity: η_M

The following sections describe the procedure of determination of unknowns by using neural network and PSO.

3.1. Overall methodology steps

The methodology for determination of the most probable set of unknown rheological parameters is as follows:

(1) generation of a database with a large number (n^3, with 'n' being the selected number of values for each parameter) of provisional input rheological parameters (G_K/K_M, η_K and η_M) sets using numerical simulations. These simulations result in n^3 output sets, which represent deformation values over certain, pre-defined, period of time;

(2) the input - output datasets are then used to develop the NetRHEO neural network ('net' standing for 'network', and 'rheo' standing for 'rheological') using a back-propagation learning algorithm. After a certain number of training iterations, the post-trained NetRHEO is expected to approximate the numerical simulations. Here, the NetRHEO is used as the response surface method to establish a link between the pre-defined ranges of rheological parameters and the long-term deformations. Within this study, the input layer and the output layer forming NetRHEO, consist only of the numerical data and not the real on-site monitoring data. Hence, the most important benefit of NetRHEO is to significantly reduce the number of numerical simulations and thus overall computation time;

(3) next step involves utilization of a Particle Swarm Optimization (PSO) algorithm, representing a form of back analysis. PSO choses the most probable set of rheological parameters (G_K/K_M, η_K and η_M) from the actual in-situ long-term monitored data, utilizing the established link between displacements and rheological parameters. The long-term monitoring is used to find the best fit curve, described by one set of parameters. The 'most probable' set of rheological parameters will be further validated in the numerical model through comparison of calculated and monitored values;

(4) the numerical analysis, now with all constitutive model parameters fully defined, are conducted to predict the behavior of soft rock mass surrounding tunnel, for a long-time period after its construction.

The behavior of a tunnel in a soft rock mass is usually time dependent, due to both the sequential construction process as well as the rheological characteristic of the rock mass. As Sharifzadeh et al. (2013) note, the major difference between creep and time-independent constitutive models is related to the time aspect of the numerical simulation. In time-independent, static analyses, a time-step is a virtual value for stepping towards the steady-state condition. In time-dependent, creep analyses, a time-step in computer code represents real time. Selection of time-step is necessary to ensure the stability of the time-dependent numerical solution. In these type of simulations, numerical steps correlate to the real construction sequences and with real period of tunnel usage, to achieve realistic model's results. The software allows the user to select a predefined time-step, where the creep constitutive laws make use of the time-step in the equations, so time-step may affect the response. However, for the system to be always in mechanical equilibrium, and to avoid rapid increase of unbalanced forces (Pellet et al., 2009), the time-dependent stress increment must not be large compared to the strain-dependent stress increment. For the selected constitutive model, a maximum creep time-step is calculated as follows:

$$\Delta t_{max}^{cr} = \min\left(\frac{\eta^K}{G^K}; \frac{\eta^M}{G^M}\right) \tag{11}$$

Within this study, the time-dependent behavior of the tunnel was simulated by running the modified Burgers model for a period of 15 years, The numerical displacements are calculated for the selected periods, once every year, with the intent to match the tunnel response as observed through monitoring.

3.2. Development of NetRHEO neural network

The neural network (NN), which usually requires a large amount of data, is a very efficient tool for determination of rheological parameters from the in-situ long-term monitoring results. Because of its numerous advantages over traditionally used statistical and experimental methods, these include; excellent information processing capability pertinent to highly non-linear problems, high parallelism, fault and noise tolerance,

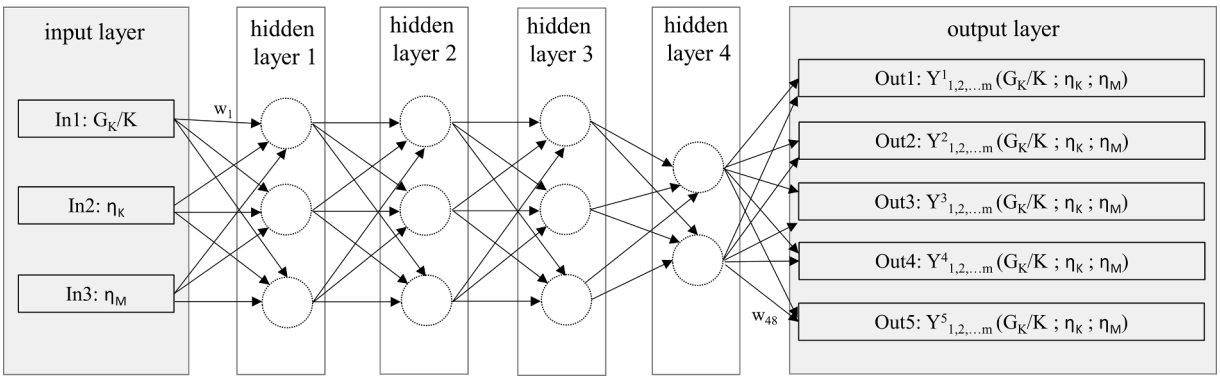

Fig. 4. A scheme of a NetRHEO neural network when considering the 5 rock mass observation points.

self-learning and generalization, many researchers utilized the benefits of NNs in rock tunneling (Lee and Sterling, 1992; Moon et al.1995; Benardos and Kaliampakos, 2004; Yoo and Kim, 2007; Mahdevari and Torabi, 2012; Guan et al., 2009; Hasegawa et al., 2019). Zhang et al. (2020c) gave an extensive state of the art review of soft computing applications in underground excavations, among which are artificial neural networks. Application of these methods is in alignment with the International Society for Soil Mechanics and Geotechnical Engineering's (ISSMGE's) latest initiative to explore machine learning methods in geotechnical engineering (Zhang et al., 2020b).

As an advanced machine learning algorithm, NN represents an alternative to the well-established pool of response surface methods (see Li et al, 2016), such is the Kriging model, used because of its recognized ability to provide high quality predictions. However, some studies (Kaewkongkaew et al., 2015) showed that ordinary Kriging does not work well in estimating rock mass quality along tunnel alignments in complex geological settings. Further, Shi et al. (2019) state that the NN surrogate model can accurately estimate the geological conditions prior to excavation when compared with the other soft computing methods, while Santos et al. (2014) conclude that model errors obtained with the different estimation methods (linear regression, geostatistical Kriging and NN algorithms) are very similar.

As an advanced machine learning technique, NN simulates the functioning of the human brain and the nerve system. To learn relationships, which are intuitively difficult to understand and describe, NN relies on sharing information between interconnected artificial neural network elements, leading to development of awareness of the relationship between different parameters (Reale et al., 2018). This study utilizes the NN regression analysis, where the network architecture of so-called Multilayer Layer Perceptron (MLP) consists of an input layer, a hidden layer(s) and an output layer. An MLP can be regarded as a directed graph consisting of multiple node layers, and each node is connected to the next layer (Zhang et al., 2020d). Extensive literature overview of methods to determine the optimal number of hidden layers and hidden nodes, influencing the NN performance, is given by Sheela and Deepa (2013). The number of input and output layer is based on the specific problem of rheological parameter determination, while the optimal number of hidden layers is optimized by involving simple manual trial and error procedure. By assigning and adapting a weighting to each neuron interconnection, the neural network prediction capabilities are developed. Based on the scheme proposed by Hammerstrom (1993), it is recommended that 70% of input- output data is used for training process in order is to find optimum neural weightings, so to minimize the error function. Once the NN is trained, the following validation includes simulation of an output data with input data, where 15% of total data is used in process. Finally, the testing phase uses remaining 15% of data to provide an unbiased evaluation of a final model fit on the training dataset. Generally, the amount of necessary dataset depends both on the complexity of problem and on the complexity of the chosen algorithm.

A neural network NetRHEO, was trained, tested and validated within this study to learn the relationships between rock mass rheological parameters and tunnel time-dependent deformations. The input set consist of 'n' values of selected rheological parameters $[(G_K/K_M)_1, (G_K/K_M)_2, \ldots, (G_K/K_M)_n]$; $[\eta_{K1}, \eta_{K2}, \ldots, \eta_{Kn}]$; $[\eta_{M1}, \eta_{M2}, \ldots, \eta_{Mn}]$. The output is determined through the n^3 numerical analysis where each observed point of rock mass surrounding the tunnel has the form of $\{[y_{t1}, y_{t2, \ldots}, y_{tm}]\}_1$; $\{[y_{t1}, y_{t2, \ldots}, y_{tm}]\}_2$; … ; $\{[y_{t1}, y_{t2, \ldots}, y_{tm}]\}_{n^3}$ with 'y' being the deformation / displacement, 't' being the observed time, and 'm' being the largest observed time. If several points of rock mass surrounding tunnel are considered for deformation / displacement evaluation, then the outputs would be in form of several matrices, namely, $\{[y^1_{t1}, y^1_{t2, \ldots}, y^1_{tm}], [y^2_{t1}, y^2_{t2, \ldots}, y^2_{tm}], \ldots, [y^z_{t1}, y^z_{t2, \ldots}, y^z_{tm}]\}_1$ to $\{[y^1_{t1}, y^1_{t2, \ldots}, y^1_{tm}], [y^2_{t1}, y^2_{t2, \ldots}, y^2_{tm}], \ldots, [y^z_{t1}, y^z_{t2, \ldots}, y^z_{tm}]\}_{n^3}$ with 'z' being the number of observed points.

For example, if the rock mass deformation / displacement is monitored in five (5) fixed points, for the definite number of 'm' times, a NetRHEO consists of three (3) input nodes and five (5) output nodes, with utilization of total 48 distinct weightings. Four hidden layers form the links between the input and the output layer. Whereas the first, second and third hidden layers consist of three nodes, while the fourth one consists of two nodes. The overall number of hidden layers, as well the number of belonging nodes in each hidden layer, is determined through a 'trial and error' method, adopting several rule-of-thumb methods described in (Sheela and Deepa, 2013). A sigmoid activation function for hidden neurons and a linear activation function for output neurons are used. A scheme of a developed neural network is given in Fig. 4.

The developed NetRHEO is further used for the estimation of most probable set of rheological parameters through utilization of PSO.

3.3. Optimization of NetRHEO by using PSO

Particle Swarm Optimization (PSO) represents a heuristic search method inspired by the swarming or collaborative behavior of biological populations. Since it was first published by Kennedy and Eberhart (1995), a PSO became very popular in different fields of human activities, and so in geotechnical engineering (Chen and Feng, 2007; Hajihassani et al., 2018). The main purpose of PSO algorithm is to propagate particles in the desired function space, leading to their placement in optimal points of this space. The particles randomly move from points to another set of points in a single iteration, with likely improvement using a combination of deterministic and probabilistic rules. Three steps need to be conducted within the PSO algorithm and these include generation of particles' positions and velocities, velocity update, and position update (Hassan et al., 2005).

As a first step, the positions, x^i_m, and velocities, v^i_m, of the intial swarm of particles are randomly generated allowing the particles to be

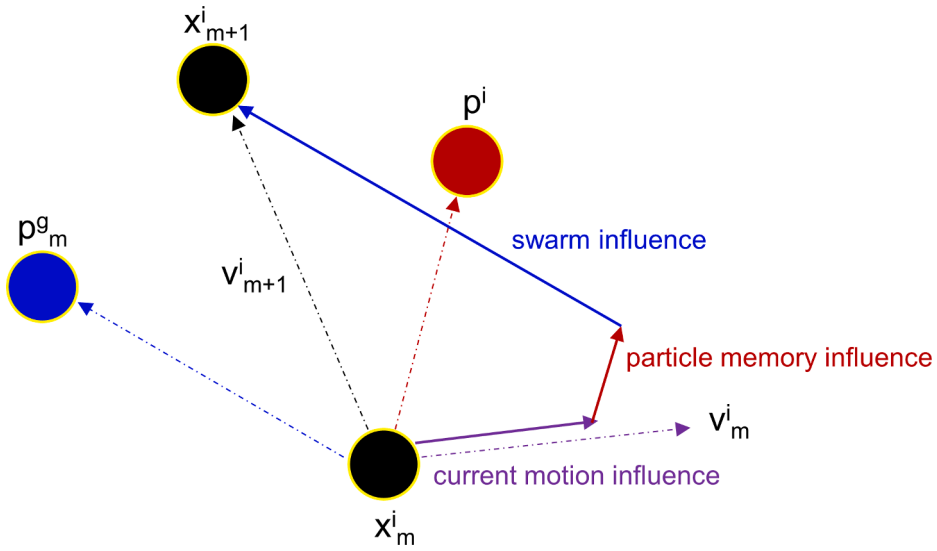

Fig. 5. A view of the velocity and position updates in Particle Swarm Optimization.

randomly distributed across the space in initial time 'm'. This is done by utilizing the upper and lower bounds of the design variables values, x_{min} and x_{max}, as given in Eqs. (12) and (13), where '*rand*' is a uniformly distributed random variable with value between 0 and 1:

$$x^i_o = x_{min} + \text{rand}(x_{max} - x_{min}) \tag{12}$$

$$v^i_o = \frac{x_{min} + \text{rand}(x_{max} - x_{min})}{\Delta t} \tag{13}$$

Next step consists of updating the velocities of all particles at time 'm + 1′, by utilizing the so called particles fitness values, representing the functions of the particles positions in the space at time 'm'. The velocity update formula uses two information determined by the particle fitness

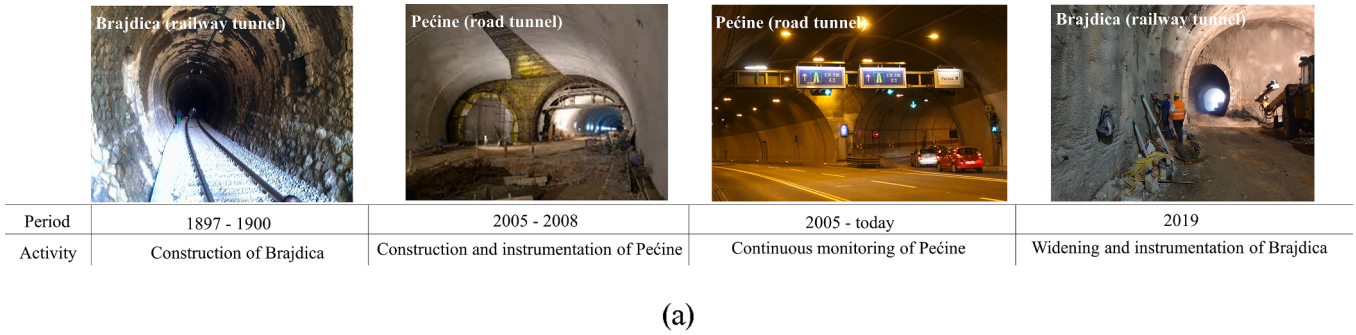

Period	1897 - 1900	2005 - 2008	2005 - today	2019
Activity	Construction of Brajdica	Construction and instrumentation of Pećine	Continuous monitoring of Pećine	Widening and instrumentation of Brajdica

(a)

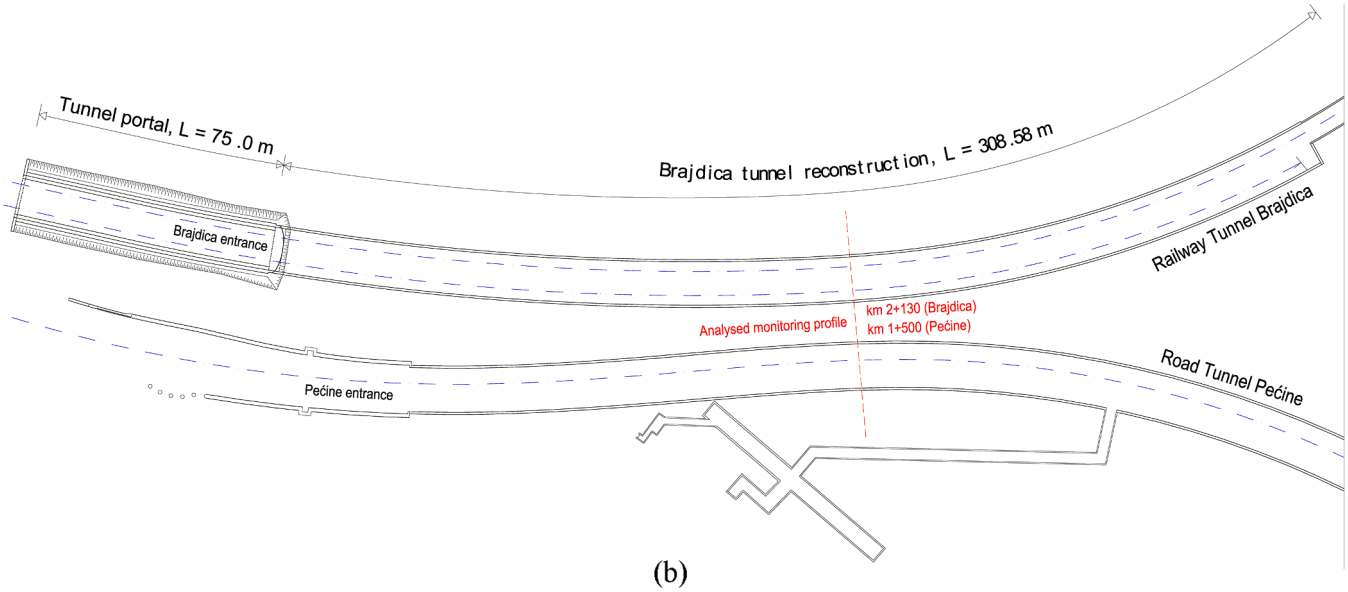

(b)

Fig. 6. Timeline of construction and monitoring (a) and layout (b) of two adjacent case study tunnels – railway tunnel Brajdica and road tunnel Pećine.

function value and these include *'which particle has the best global value, p^g_m, in the current swarm'* and *'which is the best position of each particle over time, p_i, in current and all previous moves'*. By using these information, the velocity update formula provides a search direction v^i_{m+1} for the next iteration, through following equation:

$$v^i_{m+1} = w \times v^i_m + c_1 \times \text{rand}\frac{p^i - x^i_m}{\Delta t} + c_2 \times \text{rand}\frac{p^g_m - x^i_m}{\Delta t} \quad (14)$$

where the v^i_m represents the current motion, $\frac{p^i - x^i_m}{\Delta t}$ represents particle own memory and $\frac{p^g_m - x^i_m}{\Delta t}$ represents swarm influence. Three weight factors are used in Eq. (14) and include inertia factor w, self-confidence factor c_1, and swarm confidence factor c_2. These weight factors, as well as the largest overall swarm size, have the largest influence on PSO performance (Jahed Armaghani et al., 2019). This study uses $w = 1$, $c_1 = 2$ and $c_2 = 2$, respectively, since they provide the best convergence rate for the analyzed problem. The chosen swarm size is 50 particles. A view of the velocity and position updates in Particle Swarm Optimization is given in Fig. 5.

These steps are repeated until a desired convergence criterion is met. Within this study, the stopping criteria is defined when the maximum change in best fitness is smaller than specified tolerance for a specified number of moves, S, as shown in Eq. (15). In this work, S is specified as ten moves and ε is specified as 10^{-5}.

$$\left|f\left(p^g_m\right) - f\left(p^g_{m-q}\right)\right| \le \varepsilon \text{ where } q = 1,2,\ldots,S \quad (15)$$

The algorithm code was written within the Matlab software (Mathworks, 2019).

Even though the Genetic Algorithm (GA) is often used for the task of finding the best fitting curve (Guan et al., 2009), PSO offers all of the GA advantages such as intuitiveness, ease of implementation, and the ability to effectively solve highly nonlinear, mixed integer optimization problems that are typical of complex engineering systems. Also, PSO has the same effectiveness in finding the true global optimal solution. However, GA is characterized by an expensive computational cost, while PSO offers significantly better computational efficiency (less function evaluations) by implementing statistical analysis and formal hypothesis testing. This computational efficiency superiority of PSO over the GA was proved by many authors (Hassan et al., 2005; Kaushik and Kumar, 2016).

4. Validation of the methodology: long-term behavior of tunnels Pećine and Brajdica

The efficiency of NetRHEO neural network, optimized by the particle swarm optimization algorithm for the purpose of obtaining the most probable set of rheological parameters, is validated using a case study of the two tunnels constructed next to each other in a soft karstic rock mass of Croatia.

4.1. Description of the study area

The railway tunnel Brajdica and road tunnel Pećine are located under the city of Rijeka, as one of the most important tourist and freight hubs on the 10-T Mediterranean corridor. The construction timeline for both tunnels is given in Fig. 6a. Construction of a tunnel in vicinity of the existing tunnel is a challenging task considering their possible interaction. The extensive summary of studies on the impact of construction in the vicinity of an existing tunnel is given by Chen et al. (2019), considering the impact of tunnel shape, type and different clearances.

Tunnel Brajdica is on the international railway line M603, which is part of Mediterranean corridor of the TEN-T network. It is constructed in period from 1897 to 1900 as a single-track railway tunnel with overall length of 1838 m. However, a tunnel reconstruction is of high priority, since the current operational capacity of tunnel is not sufficient, and it is currently a bottleneck asset of M603 line. The reconstruction covers widening of a tunnel profile to accommodate the new, second, track in order to increase the railway station capacity. The widening of the Brajdica tunnel which has a stone lining, is done based on NATM principles, where the new primary support includes installation of a 20 cm thick shotcrete layer, steel lattice girders at 1.5 m separation and 6 m long self-drilled steel rock bolts, with 21 rock bolt installed along the cross section. Tunnel Pećine is located on the D404 state road, and it provides direct access to the city of Rijeka and its major port area. The tunnel has an overall length of 1258.5 m, with 60% of tunnel constructed as three-lane and 40% constructed as a four-lane highway. It is constructed between 2005 and 2008. The construction of Pećine was conducted using the NATM philosophy, including blasting (in high quality rock mass sections) and mechanical excavation (in poor quality rock mass sections), with installation of monitoring equipment to observe the short-term and long-term behavior of rock mass surrounding tunnel. The primary support system of tunnel Pećine consists of a 20 cm thick shotcrete installed in several layers and 6 m long self-drilled steel rock bolts, with 23 rock bolts installed along the cross section.

The tunnel Brajdica reconstructed profile and tunnel Pećine profile are relatively close, see Fig. 6b, with smallest distance between tunnel walls of 11.4 m, corresponding to the chainage km 1 + 500 of road tunnel Pećine and km 2 + 130 of reconstructed railway tunnel Brajdica. This cross-section, representative for the tunnel portion with equal overburden depth and similar rock mass engineering-geological conditions, will be used for verification of the methodology. Overall, the case study tunnel Pećine has eight monitoring profiles in total. If other monitoring profiles are selected for verification, new numerical simulations would be necessary for each profile, in order to include additional influence of other factors affecting the long-term displacement (such as geological conditions, tunnel overburden, support strength and stiffness, vicinity of adjacent tunnel etc.). This would yield new set of input–output data for NN as surrogate model, and PSO would eventually estimate most probable set of parameters which differs from the one obtained for the tunnel section analyzed in the paper. However, the overall paper methodology presented in the paper would remain the same for all analyzed sections. Still, by treating only rheological parameters as unknowns, while the impact of other affecting factors on the long-term displacements should be evaluated with the additional numerical analysis, poses certain limitation of the presented study.

4.2. The constitutive model input parameters

The rock mass surrounding the case study tunnels is formed of cretaceous deposits, breccias, dolomites and limestones, of relatively good permeability. Therefore, the rock mass is highly susceptible to the karstification process leading to series of karstic phenomena which posed additional construction challenge, with the degree of rock mass fracturing more pronounced near the fault zones.

The rock mass parameters, used as the input for numerical analysis, are obtained by means of in-situ and laboratory investigation works prior and during the construction of tunnel Pećine, as well during the reconstruction of tunnel Brajdica. To determine Hoek-Brown's parameters (m_b, s, a), the geological strength index (GSI) is used, representing a simplified classification system based on the assessment of lithology, structure, and surface conditions of rock mass discontinuities. The GSI assessment was conducted during the excavation of both tunnels in the analyzed zone, where the GSI evaluated during the reconstruction of Brajdica tunnel is in agreement with the GSI values obtained 15 years before, during the construction of tunnel Pećine. The unconfined strength (UCS) is given as the mean value value of total of 56 triaxial, uniaxial and PLT test, while the m_i is determined as the mean result value of total 36 triaxial tests, as reported by Kovačević et al. (2020). The disturbance factor (D) in this study is defined by the input value of 0.1, considering the excavation technology of combining blasting (in high quality rock mass sections) and mechanical excavation (in poor quality rock mass sections).

To determine Maxwell parameters, K_M and G_M, the karst-adapted

Table 1
Numerical constitutive model input values.

Kelvin's parameters		Maxwell's parameters			Hoek-Brown's parameters		
G_K (MPa)	η_K (–)	K_M (MPa)	G_M (MPa)	η_M (–)	m_b (–)	s (–)	a (–)
Determined by PSO	Determined by PSO	from E_{rm}=IKs · GSI^2 · V_p ^{2}		Determined by PSO	1.870	0.001	0.500
		GSI (–)	V_p (km/s)		from rock mass parameters		
					m_i (–)	GSI (–)	UCS (MPa)
		29	0.1–4.0		7	29	60

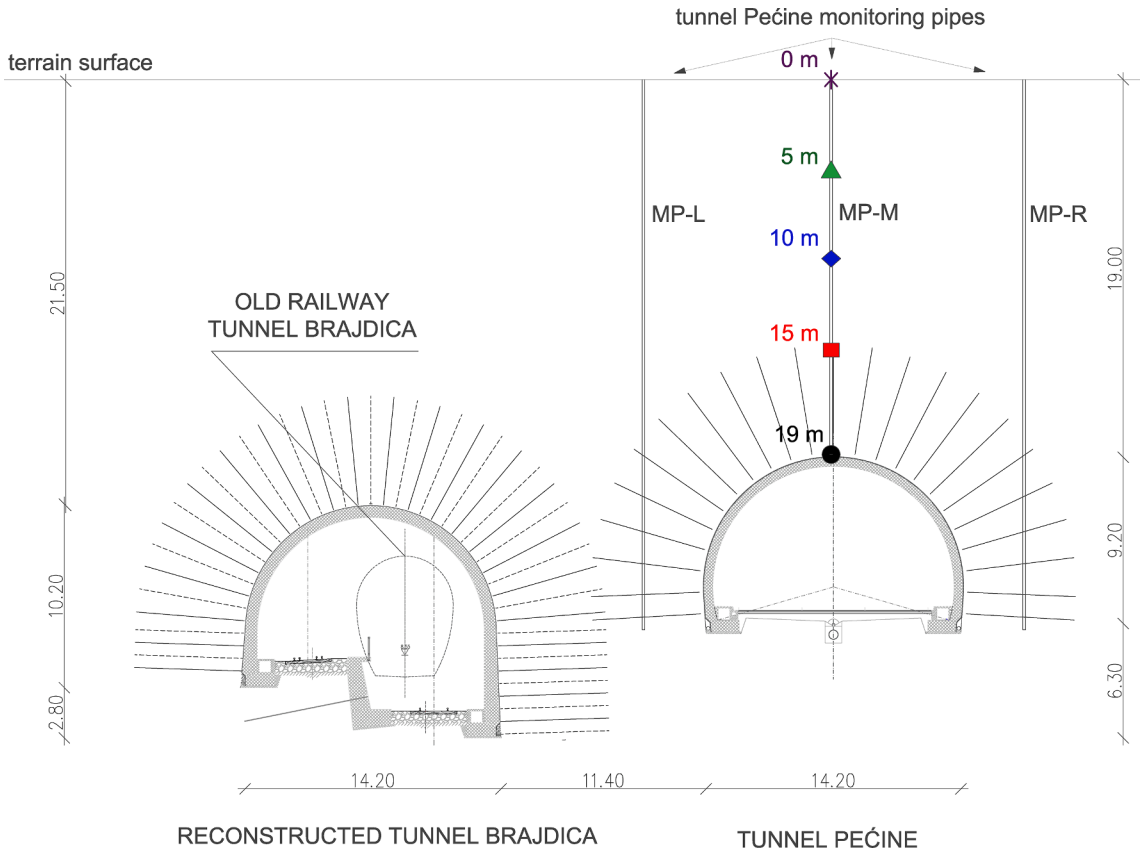

Fig. 7. The analyzed monitoring profile with installed monitoring equipment.

rock mass stiffness given by Eq. (10) is implemented. Beside the GSI value, this modulus includes, unique value 0.4 for ID_m and values of longitudinal wave velocities (V_p) determined from the seismic profile, obtained by the means of the seismic refraction method. Considering the increase of the rock mass stiffness due to the V_p increase, as given by Jurić Kaćunić et al. (2011), a FISH, programming language, code representing the non-linear increase of rock mass stiffness is implemented within the two-dimensional finite difference software FLAC (Itasca, 2019).

Maxwell parameter η_M as well as Kelvin parameters η_K and G_K (defined by the G_K/K_M ratio), representing the time-dependent behavior of rock mass, are determined by the means of NetRHEO and PSO. The overall input parameters are given in Table 1.

4.3. Long term monitoring database

During the construction of a tunnel Pećine, extensive instrumentation was employed to determine the behavior of a tunnel during the construction and in operation, Fig. 7. The monitoring activities are conducted annually from June 2005, marking the date when the analyzed cross-section of tunnel Pećine is excavated. The micrometer measurements were conducted using the measurement pipe installed from the terrain surface to the depth of tunnel crown and these provide data on vertical displacement of rock mass. Additionally, the inclinometer measurements were conducted using the measurement pipe installed from the terrain surface to the depth of tunnel bottom, from each side of tunnel, to obtain data on horizontal displacement of the rock mass. Considering that this equipment is installed in soft rock mass and is used for the continuous long-term measurements, it is important to ensure that the monitoring pipes do not move during the monitoring period in addition to the displacements caused by rock mass creep. To ensure reliable measurements, installation errors were minimized with careful installation procedures, where measurement pipes were installed in drilled boreholes, and the space between pipes and the borehole wall was filled with the cement slurry ensuring the fixed position of pipes in boreholes. Each measurement pipe was then covered with a steel cover cap and secured by the lock in terrain surface. Also, the survey point is installed at the surface, on the location of each pipe steel cap, and the annual measurements show that there are no movements of the steel cap protecting the measurement pipes. Regarding measurement errors, Dunnicliff (1988) notes that the total error measured is the sum of random errors, which include environmental errors that result in uncontrollable fluctuations of measured variables displacements, and systematic error, where the impact of random errors on the total error is

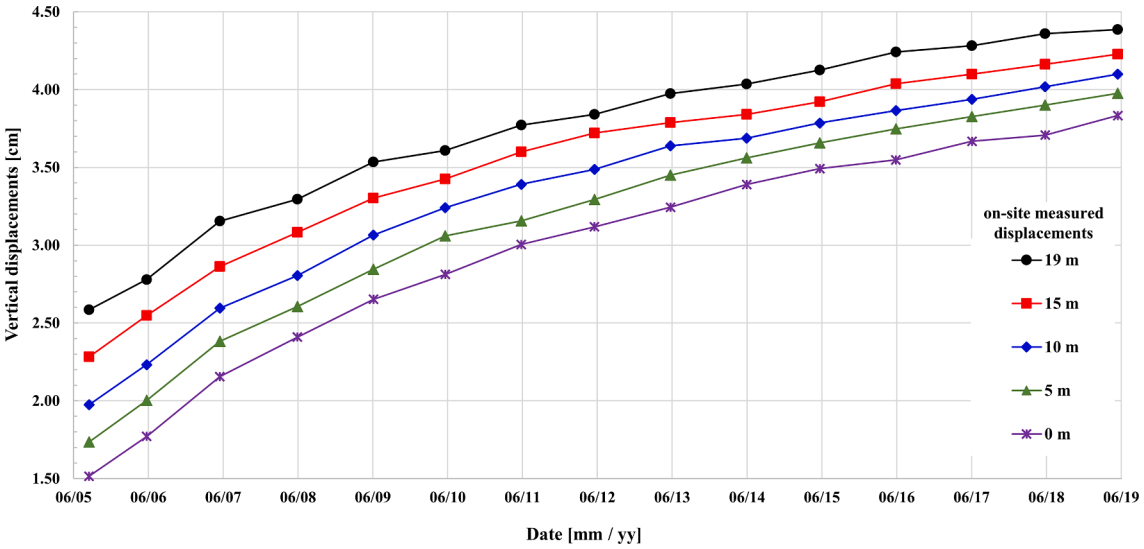

Fig. 8. Measured vertical displacement from 15 year monitoring of tunnel Pećine.

much smaller than the impact on systematic error. While random errors are only minimized through careful equipment installation, systematic errors in this study are corrected using well-known mathematical procedures.

The obtained monitoring results of vertical displacements for tunnel Pećine are shown in Fig. 8. Five measurement points are observed along the installed micrometer; first one on the terrain surface, following three on 5 m separation and the last one on the level of tunnel crown.

It should be noted that, after the construction of the mentioned section of tunnel Pećine, monitoring frequency reduced to once a year, with the data acquisition being performed and monitoring database being updated annually, in the month of June. It is clearly visible that the observed points experience similar trend of increasing vertical displacement values, albeit at a continuously reduced rate, throughout the monitoring period. As expected, the crown point experiences the largest displacement values. When compared to the short-term displacement caused by the tunnel excavation, the overall vertical displacements increased for 70% for a tunnel crown observation point, up to the 153% for the observation point on terrain surface. This study utilizes vertical displacements for the evaluation of rock mass behavior. This is in line with similar studies, for example Xiang et al. (2018), where, if the ground above the tunnel is considered, the vertical displacements are in fact dominant displacements. In this study, total displacement values are similar to the vertical displacement values, since horizontal displacement values at the same observation points are less than 8% of the vertical displacement values. Therefore, if total displacements are considered as an input, the estimated rheological parameters would not change significantly from those estimated using vertical displacements. The consideration of five observation points represents a step forward from some previous studies, such as Guan et al. (2009), which use convergence measurements of tunnel lining for the analysis of long-term behavior of a tunnel. In same time, consideration of additional observation points would add to the complexity of the neural network, while in same time would not significantly enhance the overall rheological parameter estimation procedure.

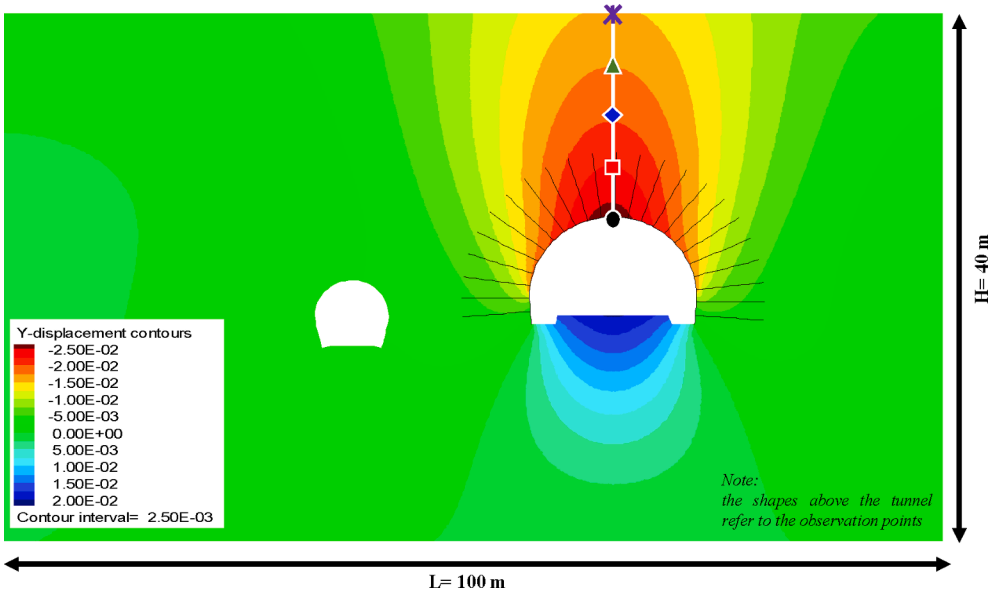

Fig. 9. Numerical model and contours of vertical displacements occurred shortly after the excavation of tunnel Pećine.

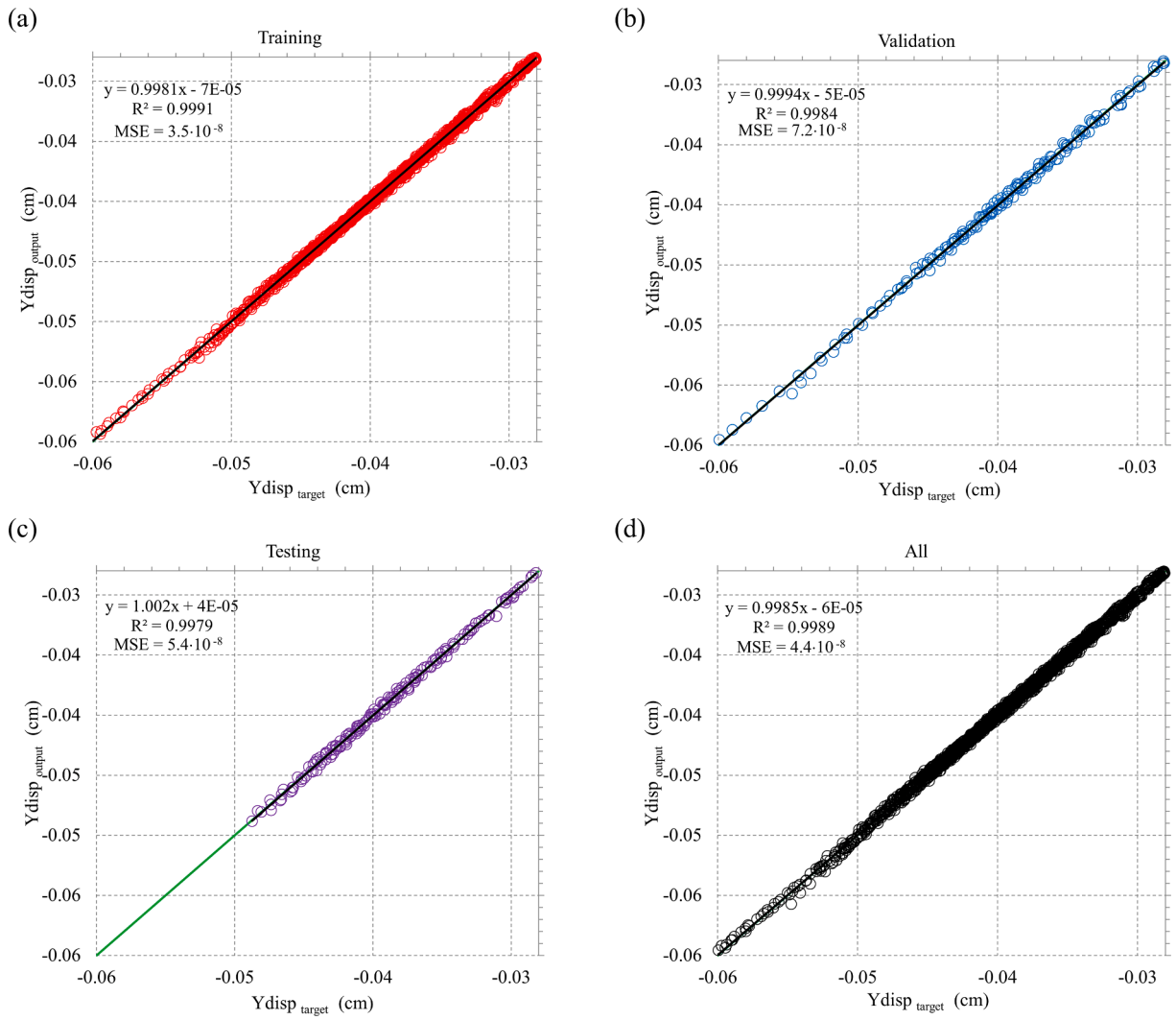

Fig. 10. Training (a), validation (b), testing (c) and overall (d) datasets with correlation of NetRHEO predicted time-dependent displacements and rheological parameters.

4.4. Application of a NetRHEO neural network

As a first step in applying the neural network, 125 (i.e. 5^3 being possible number of combinations, where '5' represents a number of predefined values for each parameter, while '3' represents number of parameters) numerical analyses were carried using the following sets of input parameters:

- Kelvin shear modulus / Elastic bulk modulus, $G_k/K_M = [0.2; 0.4; 0.6; 0.8; 1.0]$
- Kelvin viscosity, $\eta_K = [2{\cdot}10^5; 4{\cdot}10^5; 6{\cdot}10^5; 8{\cdot}10^5; 1{\cdot}10^6]$
- Maxwell viscosity, $\eta_M = [2{\cdot}10^6; 4{\cdot}10^6; 6{\cdot}10^6; 8{\cdot}10^6; 1{\cdot}10^7]$

The possible range of selected input parameters for soft rock was based on their actual range obtained from the literature (Guan et al., 2009; Weng et al., 2010; Sharifzadeh et al, 2013; Mahdevari and Bagherpour, 2014; Hamza and Stace, 2018; Paraskevopoulou and Diederichs, 2018; Wang et al., 2019; Huang et al., 2020), and the range was additionally extended, so that upper and lower boundary of each parameter range can be considered as sufficient to estimate the most probable parameter value in the subsequent analysis. These 125 sets of rheological parameters were applied to the same numerical model, which then proceeds to the calculation of long-term behavior. The input–output pair, provided by the numerical simulations, is called one dataset.

The numerical model showing the contours of vertical displacements for the period just after the excavation of tunnel Pećine, is given in Fig. 9. The figure points to the fact that excavation of Pećine has a small effect on vertical displacements of tunnel Brajdica. However, this could not be verified considering that no on-site measurements on the tunnel Brajdica were conducted during the excavation of tunnel Pećine. A sensitivity analysis was performed to check for boundary effects and a FLAC model 100 m wide and 40 m high was found to satisfy the requirements.

Duration of one numerical simulation is approximately 50 min, demonstrating the significant computational efforts of long-term calculations. Concerning that the 125 numerical simulations were conducted with all possible combination of rheological parameters, total number of displacements calculated in each observed point is 1875 (15 years × 125 calculations).

The overall matrix output has form:

$\{[y^1_1, y^1_2, \ldots, y^1_{15}], [y^2_1, y^2_2, \ldots, y^2_{15}], \ldots, [y^5_1, y^5_2, \ldots, y^5_{15}]\}_1$
$\{[y^1_1, y^1_2, \ldots, y^1_{15}], [y^2_1, y^2_2, \ldots, y^2_{15}], \ldots, [y^5_1, y^5_2, \ldots, y^5_{15}]\}_2$
…
$\{[y^1_1, y^1_2, \ldots, y^1_{15}], [y^2_1, y^2_2, \ldots, y^2_{15}], \ldots, [y^5_1, y^5_2, \ldots, y^5_{15}]\}_{125}$

where each of 125 NetRHEO outputs contain 5 sets of vertical displacements of observed points, calculated for period of 15 years. These 125 input–output datasets were used for training, testing and validating the NetRHEO neural network. The complete input–output datasets are

Table 2
Results of PSO and GA optimization.

	Particle Swarm Optimization (PSO)	Genetic Algorithm (GA)
G_K/K_M (–)	0.5639	0.5732
η_K (–)	669,861	675,382
η_M (–)	5,798,236	5,832,913
f_{min}	$1.2597 \cdot 10^{-8}$	$1.7823 \cdot 10^{-8}$

given as supplementary research data of this paper (see 'Supplementary research data - NN construction database').

Within the 'trial and error' method, 32 different neural network architectures were evaluated. Obtained R^2 and MSE values for each architecture are given as supplementary research data of this paper (see 'Supplementary research data - NN trial and error database'). Fig. 10 shows the regression coefficients for training, testing and validation and overall datasets, determined for vertical displacement, for the selected NetRHEO architecture, shown on Fig. 4. The R^2 values for the target-output evaluations are basically equal to unity, confirming that the NetRHEO established strong correlation between time-dependent displacements and rheological parameters. Regarding the mean square error for the target-output evaluations, it yields the following values: $3.5 \cdot 10^{-8}$ for training dataset, $7.2 \cdot 10^{-8}$ for validation dataset, $5.4 \cdot 10^{-8}$ for testing datase and $4.4 \cdot 10^{-8}$ for overall dataset. This efficiency of NetRHEO in establishing the complex, non-linear, relationship is expected, having in mind that NetRHEO is basically describing the Burgers constitutive model, i.e. rheological parameter – displacement correlation. Since the main goal of neural network is to learn a function to map input data to output data, The obtained high values of R^2 and low values of MSE for training, validation, testing and overall data, prove that the chosen number of input combinations is representative.

4.5. PSO estimation of most probable set of rheological parameters

The post-trained network is employed to estimate the most probable set of rheological parameters via a genetic algorithm (GA) and particle

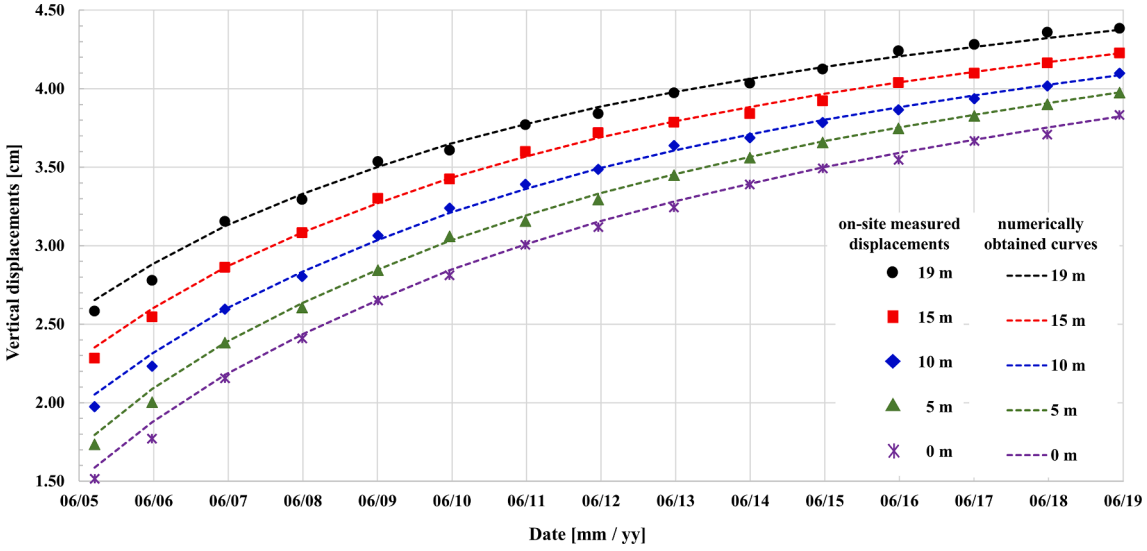

Fig. 11. Numerically obtained vertical displacements for tunnel Pećine during the period of 15 years.

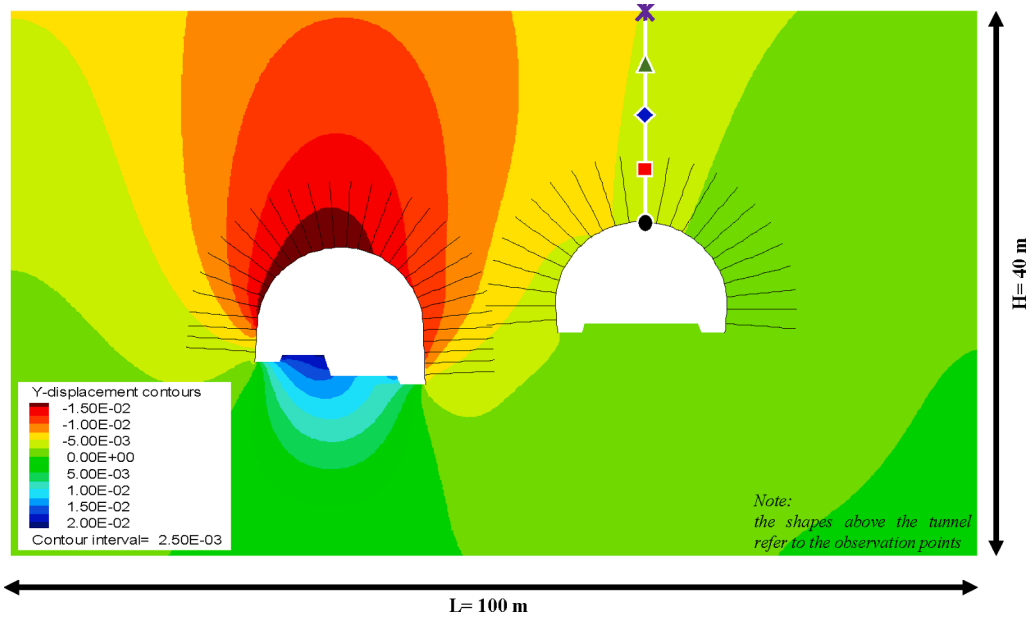

Fig. 12. Numerical model and contours of vertical displacements occurred shortly after the reconstruction of tunnel Brajdica.

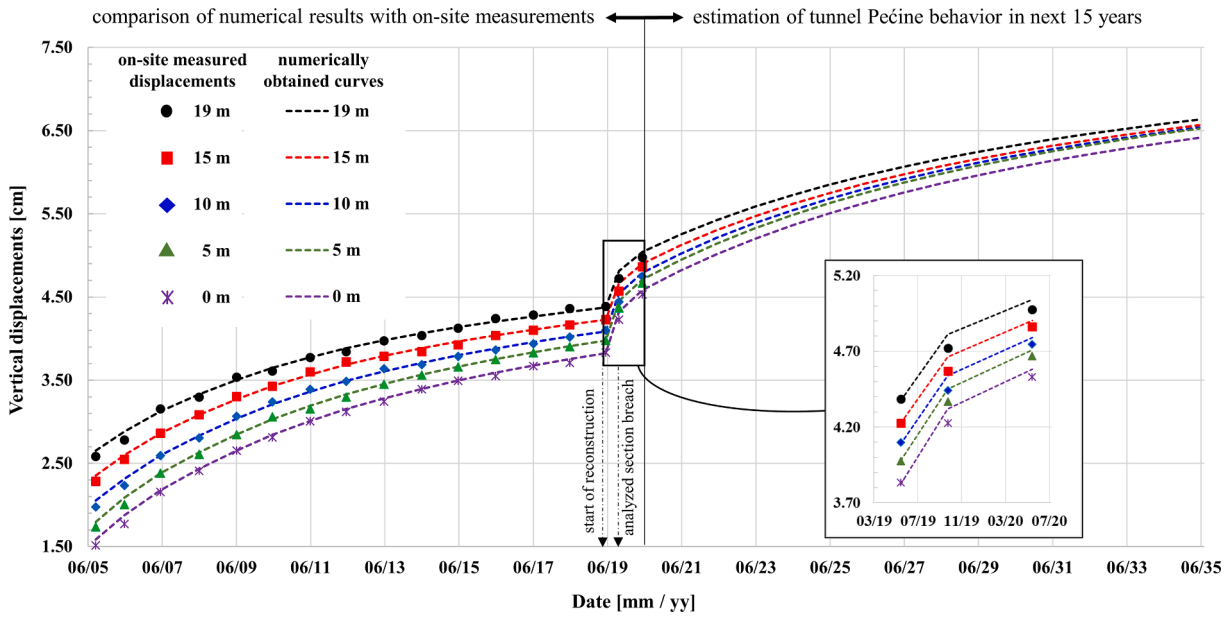

Fig. 13. The increase of vertical displacement of tunnel Pećine crown: simulated and monitored values from period of June 2005 to June 2020 (left panel) and numerically predicted values for period up to 2035 (right panel).

swarm optimization (PSO) algorithm code, implemented in MATLAB (Mathworks, 2019). As an input, monitoring data from five observed points, shown on Fig. 8, are used. The main goal of both the GA and PSO is to find the minimum value of a function which serves as an estimator of most probable set of rheological parameters. Therefore, these techniques are used for minimizing the sum-square-error between the network output and the desired output obtained by displacement measurements. The sum-square-error is a measure of the quality of an estimator, it is always non-negative, and values closer to zero are better. The results are shown in Table 2. When compared to the estimation results using the GA, the PSO yields three times lower value of the minimum of estimation function (f_{min}).

Inclusion of the determined best estimated rheological parameters as an input for numerical analysis, yielded the results shown in Fig. 11. It is clearly visible that, for all five observed points, numerically obtained displacement trend correlates well with the monitoring results. This validates the overall methodology of using a developed, PSO optimized, NetRHEO neural network for the estimation the most probable set of rheological parameters.

4.6. *Quantification of tunnel Brajdica reconstruction impact on tunnel Pećine displacements*

During the recent reconstruction of a railway tunnel Brajdica, a justified concern arose on the impact of excavation works on the adjacent road tunnel Pećine which operates continuously for last 12 years. The numerical model showing contours of vertical displacement just after the reconstruction of tunnel Brajdica are shown in Fig. 12.

The reconstruction works on tunnel Brajdica began in June 2019, while the breach of the instrumented section, analyzed within this paper and shown in Fig. 7, occurred during the October 2019. The micrometer measurements of the vertical displacement of adjacent tunnel Pećine showed that an abrupt increase of displacement values occurred after the excavation of tunnel Brajdica, see Fig. 13.

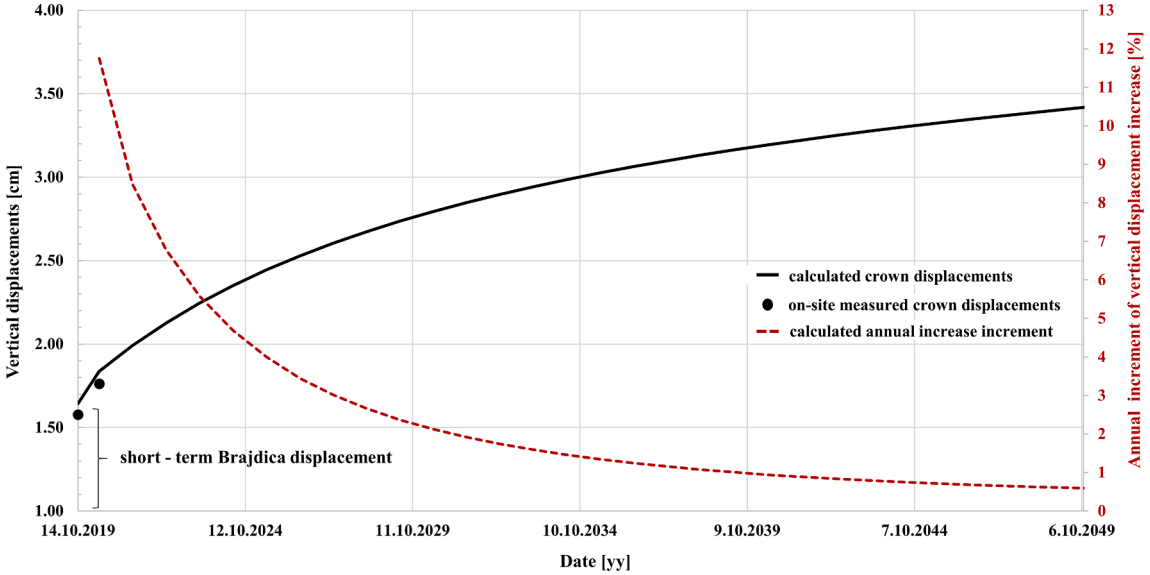

Fig. 14. Prediction of a crown vertical displacement for tunnel Brajdica, throughout the period of 30 years.

After the excavation of tunnel Brajdica, the vertical displacement values of tunnel Pećine increased around 8% for the tunnel crown point, while the surface terrain point displacement increased by 10%. These are much higher increase compared to the increase of vertical displacement during the last year prior to tunnel Brajdica excavation works, which was 0.5% for crown point and 1% for terrain surface point. The measured vertical displacement in June 2020, approximately 8 months after the excavation of the tunnel Brajdica analyzed section, shows an increase of 5% for the crown point and 6% for the terrain surface point, when compared to the data from October 2019 measured just after the excavation.

The numerical analysis show very good agreement with the monitoring results for the same period of June 2019 to June 2020, Fig. 13, where the influence of the tunnel Brajdica excavation on the tunnel Pećine displacement is calculated with high accuracy for all five observed points. After the abrupt increase due to tunnel Brajdica excavation, the numerically obtained curves for the period of next 15 years, up to year 2035, are shown in the right panel of Fig. 13. The increment of vertical displacement is similar to the one recorded before the tunnel Brajdica reconstruction. The increase in vertical displacement is further observed with the prediction of crown vertical displacement in 2035 being 39% larger than the displacement from June 2020. In same time, a terrain surface point will exhibit 48% larger value when compared to the one from June 2020.

4.7. Estimation of tunnel Brajdica long-term deformation

The established numerical model, whose reliability was validated by aforementioned comparison with the in-situ monitoring results, is further used to calculate the long-term vertical displacement of reconstructed railway tunnel Brajdica. The observed period extends to 30 years after the reconstruction. The predicted vertical displacement of a tunnel Brajdica crown is given on Fig. 14.

The numerical outputs suggest that, after the short-term crown displacement of 16 mm caused by the excavation, a vertical displacement will continue to increase in next 30 years up to a value 125% larger than the short-term displacement caused by the excavation works. Of course, this increase owes to the omnipresent long-term deformations of a tunnel in soft karstic rock. In same time, annual increment of displacement increase will gradually decrease to the value of 0.5% per year of tunnel operation.

The geodetic on-site measurements of tunnel Brajdica crown displacement correlate well with the calculated values, both for October 2019 (shortly after the excavation of analyzed section) and in June 2020.

5. Conclusions

To overcome the complex evaluation of time-dependent rheological parameters, required for the numerical calculation of long-term behavior or tunnels, this paper offers a methodology based on application of neural networks optimized by the particle swarm algorithm. Currently, the evaluation of these parameters mostly relies on costly and time-consuming laboratory tests. A NetRHEO is trained, validated and tested on the large amount of input – output sets obtained from the numerical analyses, which utilize the modified Burger's constitutive model for the description of rock mass long-term behavior, where this study utilizes Hoek-Brown criteria for the plastic component of model. Three rheological unknowns are highlighted within this study, and these include ratio of Kelvin's shear modulus and Maxwell's bulk modulus (G_K/K_M), Kelvin's viscosity (η_K) and Maxwell's viscosity (η_M). Such developed neural network is capable of estimating the most probable set of unknown rheological parameters by using the long-term monitoring database as an input. Therefore, a developed neural network NetRHEO takes full advantage of database consisting of the continuous monitoring of long-term performance of tunnels constructed in soft rock masses. To ensure most reliable estimation, a particle swarm algorithm optimization is proposed, which can offer significantly better computational efficiency in comparison to genetic algorithm, by implementing statistical analysis and formal hypothesis testing. To increase the estimation precision, several monitoring observation points are suggested within this study, covering the tunneling influence zone from terrain surface to the tunnel depth.

The overall methodology is verified on a case study location in Croatia, where the long – term monitoring data of a road tunnel Pećine was used to evaluate its complex interaction with the adjacent 100 years old railway tunnel Brajdica, recently undergone the cross section widening reconstruction. The developed, PSO optimized, NetRHEO provided a set of rheological parameters which enabled both numerical simulation of monitoring database, as well the prediction of the behavior of both tunnels throughout their service life. Such calibrated numerical model gave crucial insight on both short-term and long-term interaction of these adjacent tunnels. Therefore, it is of paramount importance for tunnel managers to understand that the instrumentation of their assets will yield numerous benefits, providing them an information on long-term tunnel resilience to rock mass creep.

CRediT authorship contribution statement

Meho Saša Kovačević: Conceptualization, Methodology, Software, Investigation, Formal analysis, Supervision. **Mario Bačić:** Conceptualization, Methodology, Investigation, Formal analysis, Visualization, Writing - original draft. **Kenneth Gavin:** Investigation, Formal analysis, Validation, Writing - review & editing. **Irina Stipanović:** Visualization, Validation, Writing - review & editing.

Declaration of Competing Interest

None.

Acknowledgements

Authors gratefully acknowledge the support from the H2020 Programme for SAFE-10-T project (Safety of Transport Infrastructure on the TEN-T Network), funded under H2020-MG-2016-2017 - Mobility for Growth call, grant agreement No 723254.

Appendix A. Supplementary material

Supplementary data to this article can be found online at https://doi.org/10.1016/j.tust.2021.103838.

References

Arapov, I., Kovačević, M.S., Lušo, P., 2009. Monitoring and Back Numerical Analyses in the Konjsko Tunnel. In: Proceedings of the Regional Symposium of the International Society for Rock Mechanics (ISRM): Rock Engineering in Difficult Ground Conditions - Soft Rocks and Karst, Amsterdam; Leiden: Balkema; CRC Press, pp. 533-538.

Aydan, Ö., Ito, T., Özbay, U., Kwasniewski, M., Shariar, K., Okuno, T., Özgenoğlu, A., Malan, D., Okada, T., 2014. ISRM Suggested Methods for Determining the Creep Characteristics of Rock. Rock Mech. Rock Eng. 47 (1), 275–290. https://doi.org/10.1007/s00603-013-0520-6.

Barla, G., Bonini, M., Debernardi, D., 2008. Time dependent deformations in squeezing tunnels. In: Proceedings of 12th International Conference of International Association for Computer Methods and Advances in Geomechanics (IACMAG), Goa, India, 1-11.

Benardos, A., Kaliampakos, D., 2004. Modelling TBM performance with artificial neural networks. Tunn. Undergr. Sp. Tech. 19 (6), 597–605. https://doi.org/10.1016/j.tust.2004.02.128.

Boidy, E., Bouvard, A., Pellet, F., 2002. Back analysis of time-dependent behaviour of a test gallery in claystone. Tunnel. Underground Space Technol. 17 (4), 415–424. https://doi.org/10.1016/s0886-7798(02)00066-4.

Carranza - Torres, C., Fairhurst, C., 1999. The elastoplastic response of underground excavation in rock masses that satisfy the Hoek-Brown failure criterion. Int. J. Rock Mech. Min. Sci. 36 (6), 777-809, 10.1016/S0148-9062(99)00047-9.

CEN: European Committee for Standardization, 2004. EN 1997-1:2004: Eurocode 7: Geotechnical design - 1. part: General Rules, European Standard, CEN, Brussels.

Chen, B.-R., Feng, X.-T., 2007. CSV-PSO and Its Application in Geotechnical Engineering. In: Swarm Intelligence Focus on Ant and Particle Swarm Optimization, IntechOpen, 548 p., 10.5772/5108.
Chen, F., Wang, L., Zhang, W., 2019. Reliability assessment on stability of Tunneling perpendicularly beneath an existing tunnel considering spatial variabilities of rock mass properties. Tunnel. Undergr. Space Technol. 88, 276–289. https://doi.org/10.1016/j.tust.2019.03.013.
Deb, D., 2010. Finite Element Method: Concepts and Applications in Geomechanics. PHI Learning Pvt. Ltd., New Delhi, India, p. 360.
Dunnicliff, J., 1988. Geotechnical Instrumentation for Monitoring Field Performance. John Wiley & Sons, New York, USA.
Fabre, G., Pellet, F., 2006. Creep and time-dependent damage in argillaceous rocks. Int. J. Rock Mech. Min. Sci. 43 (6), 950–960. https://doi.org/10.1016/j.ijrmms.2006.02.004.
Goh, A.T.C., Zhang, W., Zhang, Y., Xiao, Y., Xiang, Y., 2016. Determination of earth pressure balance tunnel-related maximum surface settlement: a multivariate adaptive regression splines approach. Bull. Eng. Geol. Environ. 77 (2), 489–500. https://doi.org/10.1007/s10064-016-0937-8.
Grimstad, E., 2001. Behaviour of steel fibre reinforced shotcrete during large deformations in squeezing rock. In: Shotcrete: Engineering Developments. CRC Press, pp. 119–122.
Guan, Z., Jiang, Y., Tanabashi, Y., Huang, H., 2008. A new rheological model and its application in Mountain Tunneling. Tunn. Undergr. Sp. Tech. 23 (3), 292–299. https://doi.org/10.1016/j.tust.2007.06.003.
Guan, Z., Jiang, Y., Tanabashi, Y., 2009. Rheological parameter estimation for the prediction of long-term deformations in conventional tunneling. Tunn. Undergr. Sp. Tech. 24 (3), 250–259. https://doi.org/10.1016/j.tust.2008.08.001.
Hajihassani, M., Jahed Armaghani, D., Kalatehjari, R., 2018. Applications of Particle Swarm Optimization in Geotechnical Engineering: A Comprehensive Review. Geotech. Geol. Eng. 36 (2), 705–722. https://doi.org/10.1007/s10706-017-0356-z.
Hammerstrom, D., 1993. Neural networks at work. IEEE Spectr. 30 (6), 26–32. https://doi.org/10.1109/6.214579.
Hamza, O., Stace, R., 2018. Creep properties of intact and fractured muddy siltstone. Int. J. Rock Mech. Min. Sci. 106, 109–116. https://doi.org/10.1016/j.ijrmms.2018.03.006.
Hasegawa, N., Hasegawa, S., Kitaoka, T., Ohtsu, H., 2019. Applicability of Neural Network in Rock Classification of Mountain Tunnel. Mater. Trans. 60 (5), 758–764. https://doi.org/10.2320/matertrans.Z-M2019809.
Hassan, R., Cohanim, B., de Weck, O., Venter, G., 2005. A Comparison of Particle Swarm Optimization and the Genetic Algorithm. In: Proceedings of 46th AIAA/ASME/ASCE/AHS/ASC Structures, Structural Dynamics and Materials Conference, Austin, Texas, USA, AIAA 2005-1897, 10.2514/6.2005-1897.
Hoek, E., Carranza - Torres, C., Corkum, B., 2002. Hoek-Brown failure criterion. In: Proceedings of 5th North American Rock Mechanics Symposium and 17th Tunneling Association of Canada: NARMS-TAC, Toronto, Canada, 267-273.
Huang, M., Zhan, J.W., Xu, C.S., Jiang, S., 2020. New Creep Constitutive Model for Soft Rocks and Its Application in the Prediction of Time-Dependent Deformation in Tunnels. Int. J. Geomech. 20 (7), 04020096. https://doi.org/10.1061/(asce)gm.1943-5622.0001663.
Itasca, 2019. FLAC Manual, section Creep Material Models. Itasca Consulting Group Inc., Minneapolis, Minnesota, USA.
Jahed Armaghani, D., Koopialipoor, M., Marto, A., Yagiz, S., 2019. Application of several optimization techniques for estimating TBM advance rate in granitic rocks. J. Rock Mech. Geotech. Eng. 11 (4), 779–789. https://doi.org/10.1016/j.jrmge.2019.01.002.
Jin, J., Cristescu, N., 1998. An elastic / viscoplastic model for transient creep of rock salt. Int. J. Plast. 14 (1–3), 85–107. https://doi.org/10.1016/S0749-6419(97)00042-9.
Jurić Kaćunić, D., Arapov, I., Kovačević, M.S., 2011. New approach to the determination of stiffness of carbonate rocks in Croatian karst. Građevinar 63 (2), 177–185.
Kaewkongkaew, K., Phien-wej, N., Kham-ai, D., 2015. Prediction of rock mass along tunnels by geostatistics. KSCE J. Civ. Eng. 19, 81–90. https://doi.org/10.1007/s12205-014-0505-3.
Kaushik, A., Kumar, H., 2016. Performance Evaluation between GA versus PSO. Int. Res. J. Eng. Technol. 3 (6), 103–110.
Kennedy, J., Eberhart, R., 1995. Particle Swarm Optimization. In: Proceedings of the IEEE International Conference on Neural Networks, University of Western Australia, Perth, Australia, 1942-1945.
Kovačević, M.S., Jurić-Kaćunić, D., Simović, R., 2011. Determination of strain modulus for carbonate rocks in Croatian karst. Građevinar 63 (1), 35–41.
Kovačević, M.S., Gavin, K., Stipanović Oslaković, I., Librić, L. 2018. Monitoring of long term deformations in Bobova tunnel. In: Proceedings of the 5th International Conference on Road and Rail Infrastructure (CETRA), Zadar, Croatia, 1507-1514, 10.5592/CO/cetra.2018.844.
Kovačević, M.S., Bačić, M., Gavin, K., 2020. Application of Neural Networks for the Reliability Design of a Tunnel in Karst Rock Mass. Canad. Geotech. J., published online,. https://doi.org/10.1139/cgj-2019-0693.
Lee, C., Sterling, R., 1992. Identifying probable failure modes for underground openings using a neural network. Int. J. Rock Mech. Min. Sci. Geomech. Abstr. 29 (1), 49–67. https://doi.org/10.1016/0148-9062(92)91044-6.
Li, Y., Xia, C., 2000. Time-dependent tests on intact rocks in uniaxial compression. Int. J. Rock Mech. Min. Sci. 37 (3), 467–475. https://doi.org/10.1016/S1365-1609(99)00073-8.
Li, D.-Q., Zheng, D., Cao, Z.-J., Tang, X.-S., Phoon, K.-K., 2016. Response surface methods for slope reliability analysis: Review and comparison. Eng. Geol. 203, 3–14. https://doi.org/10.1016/j.enggeo.2015.09.003.
Lv, S., Wang, W., Liu, H., 2019. A Creep Damage Constitutive Model for a Rock Mass with Nonpersistent Joints under Uniaxial Compression. Math. Prob. in Eng. ID 4361458. https://doi.org/10.1155/2019/4361458.
Mahdevari, S., Torabi, S.R., 2012. Prediction of tunnel convergence using Artificial Neural Networks. Tunn. Undergr. Sp. Tech. 28 (1), 218–228. https://doi.org/10.1016/j.tust.2011.11.002.
Mahdevari, S., Bagherpour, R., 2014. Considering creep parameters of rock mass to evaluate the necessity thrust for excavation in squeezing ground. J. Civil Eng. Urban. 4 (4), 370–377.
Maranini, E., Brignoli, E., 1999. Creep behaviour of a weak rock: experimental characterization. Int. J. Rock Mech. Min. Sci. 36 (1), 127–138. https://doi.org/10.1016/S0148-9062(98)00171-5.
MathWorks, 2019. Matlab software. MathWorks, Natick, Massachusetts, USA.
Moon, H.K., Na, S.M., Lee, C.W., 1995. Artificial neural-network integrated with expert-system for preliminary design of tunnels and slopes. In: Proceedings of 8th Int. Congress on Rock Mechanics, Rotterdam: Balkema, 901-905.
Okui, Y., Tsuruhara, T., Ohta, H., Tada, M., Sakuma, S., Nakata, C., Seuoka, M., 2012. Case Study of Huge Squeezing Behavior in Expressway Tunnel in Service. In: Harmonising Rock Engineering and the Environment. Taylor and Francis Group, London, pp. 660–661.
Oreste, P.P., 2003. Analysis of structural interaction in tunnels using convergence-confinement approach. Tunn. Undergr. Sp. Tech. 18 (4), 347–363. https://doi.org/10.1016/S0886-7798(03)00004-X.
Paraskevopoulou, C., Diederichs, M., 2018. Analysis of time-dependent deformation in tunnels using the Convergence-Confinement Method. Tunnel. Underground Space Technol. 71, 62–80. https://doi.org/10.1016/j.tust.2017.07.001.
Pellet, F., Hajdu, A., Deleruyelle, F., Besnus, F., 2005. A viscoplastic model including anisotropic damage for the time dependent behaviour of rock. Int. J. Numer. Anal. Meth. Geomech. 29 (9), 941–970. https://doi.org/10.1002/nag.450.
Pellet, F., Roosefid, M., Deleruyelle, F., 2009. On the 3D numerical modelling of the time-dependent development of the damage zone around underground galleries during and after excavation. Tunnel. Underground Space Technol. 24, 665–674. https://doi.org/10.1016/j.tust.2009.07.002.
Pollak, D., 2007. Influence of Carbonate Rock Masses on Their Engineering-Geological Properties (In Croatian). Doctoral thesis, Faculty of Mining, Geology and Petroleum Engineering. University of Zagreb.
Reale, C., Gavin, K., Librić, L., Jurić-Kaćunić, D., 2018. Automatic classification of fine-grained soils using CPT measurements and Artificial Neural Networks. Adv. Eng. Inform. 36, 207–215. https://doi.org/10.1016/j.aei.2018.04.003.
Santos, V., Da Silva, A.P.F., Brito, M.G., 2014. Prediction of RMR Ahead Excavation Front in D&B Tunneling. In: Proceedings of the IAGE XII Congress, Torino, Italy, 15–19 September 2014, Springer International Publishing: Cham, Switzerland, 415–419, 10.1007/978-3-319-09060-3_72.
Schubert, W., Button, E.A., Sellner, P.J., Solak, T., 2003. Analysis of time dependent displacements of tunnels. Felsbau 21 (5), 96–103.
Shao, J., Chau, K., Feng, X., 2006. Modeling of anisotropic damage and creep deformation in brittle rocks. Int. J. Rock Mech. Min. Sci. 43 (4), 582–592. https://doi.org/10.1016/j.ijrmms.2005.10.004.
Sharifzadeh, M., Tarifard, A., Moridi, M.A., 2013. Time-dependent behavior of tunnel lining in weak rock mass based on displacement back analysis method. Tunnel. Underground Space Technol. 38, 348–356. https://doi.org/10.1016/j.tust.2013.07.014.
Sheela, K.G., Deepa, S.N., 2013. Review on methods to fix number of hidden neurons in neural networks. Math. Probl. Eng.: Article ID 425740, 10.1155/2013/425740.
Shi, M., Sun, W., Zhang, T., Liu, Y., Wang, S., Song, X., 2019. Geology prediction based on operation data of TBM: comparison between deep neural network and soft computing methods. In: Proceeding of the 1st International Conference on Industrial Artificial Intelligence (IAI), Shenyang, China, 23-27 July 2019. Institute of Electrical and Electronics Engineers, New York. Available from www.ieeexplore.ieee.org [accessed 10 June 2020].
Wang, X.-F., Jiang, B.-S., Zhang, Q., Lu, M.-M., Chen, M., 2019. Analytical solution of circular tunnel in elastic-viscoplastic rock mass. Latin Am. J. Solids Struct. 16 (6), e210 https://doi.org/10.1590/1679-78255701.
Weng, M.C., Tsai, L.S., Liao, C.Y., Jeng, F.S., 2010. Numerical modeling of tunnel excavation in weak sandstone using a time-dependent anisotropic degradation model. Tunnel. Underground Space Technol. 25 (4), 397–406. https://doi.org/10.1016/j.tust.2010.02.004.
Xiang, Y., Liu, H., Zhang, W., Chu, J., Zhou, D., Xiao, Y., 2018. Application of transparent soil model test and DEM simulation in study of tunnel failure mechanism. Tunnel. Underground Space Technol. 74, 178–184. https://doi.org/10.1016/j.tust.2018.01.020.
Xu, T., Tang, C., Zhao, J., 2012. Modeling of Rheological Deformation of Inhomogeneous Rock and Associated Time-Dependent Response of Tunnels. Int. J. Geomechanics 12 (2), 147–159. https://doi.org/10.1061/(ASCE)GM.1943-5622.0000130.
Xue, L., Siqing, Q., Pei, L., Guoliang, L., Adewuyi Oyediran, I., Pan, X., 2014. New quantitative displacement criteria for slope deformation process: From the onset of the accelerating creep to brittle rupture and final failure. Eng. Geol. 182 (Part A) (2014), 79-87, 10.1016/j.enggeo.2014.08.007.
Yoo, C., Kim, J.-M., 2007. Tunneling performance prediction using an integrated GIS and neural network. Comput. Geotech. 34 (1), 19–30. https://doi.org/10.1016/j.compgeo.2006.08.007.
Zhang, W., Li, Y., Wu, C., Li, H., Goh, A., Lin, H., 2020a. Prediction of lining response for twin tunnels constructed in anisotropic clay using machine learning techniques. Underground Space, published online,. https://doi.org/10.1016/j.undsp.2020.02.007.

Zhang, W., Wu, C., Zhong, H., Li, Y., Wang, L., 2020b. Prediction of undrained shear strength using extreme gradient boosting and random forest based on Bayesian optimization. Geosci. Front., published online. https://doi.org/10.1016/j.gsf.2020.03.007.

Zhang, W., Zhang, R., Wu, C., Chee Goh, A.T., Lacasse, S., Liu, Z., Liu, H., 2020c. State-of-the-art review of soft computing applications in underground excavations. Geosci. Front. 11 (4), 1095–1106. https://doi.org/10.1016/j.gsf.2019.12.003.

Zhang, R., Wu, C., Goh, A.C., Böhlke, T., Zhang, W., 2020d. Estimation of diaphragm wall deflections for deep braced excavation in anisotropic clays using ensemble learning. Geosci. Front., published online,. https://doi.org/10.1016/j.gsf.2020.03.003.